IJFANS INTERNATIONAL JOURNAL OF FOOD AND NUTRITIONAL SCIENCES
ISSN PRINT 2319 1775 Online 2320 7876
Research paper **Volume 10, Iss 3, 2021**

Design and Analysis of Bi-Directional DC-DC Driver for Electric VehiclesUsingArtificial Neural Networks

Mr.Bosubabu Sambana[1]

[1]Assistant Professor, Department of Computer Science and Engineering,
[1]Raghu Engineering College (A), Visakhapatnam, JNTU Kakinada, Andhra Pradesh, India.
ORCID: 0000-0002-8665-9441

Mr.Kuppireddy Krishna Reddy[2]

[2]Associate Professor, Department of Electrical and Electronics Engineering,
[2]Mother Theresa Institute of Engineering & Technology, Palamaner, Andhra Pradesh, India.
ORCID:0009-0000-8855-7863

***Abstract*—A bidirectional power converter for an electric car was the subject of this article, which focused on its design and modelling. Batteries, a bidirectional dc-dc converter, and a dc machine make up the power electronics block. In this study, we work to enhance the dynamic performance of a bidirectional dc-dc converter. Additionally, an innovative control strategy is discussed that uses ANN algorithms to regulate the input voltage adaptively. The first step in the process of operating the DC-DC converter through an ANN algorithm is the classification of adaptive input voltages. The voltages are then anticipated. These voltage levels are used in several simulators. To sum up, the suggested approach is very efficient and effective. Torque readings of a dc machine run in rotor and generator modes are used to identify the power converter's mode of operation. It has been ensured that the battery charging and discharging cycles are managed in accordance with the various dc machine modes of operation.**

Keywords—electricvehicle,dcmachine,bi-directionaldc-dcconverter,ANNcontrol

I INTRODUCTION

The transportation industry is a crucial part of modern society. Greenhouse gases including carbon dioxide, carbon monoxide, and methane are produced when fossil fuels are used in outdated vehicle equipment. Air pollution, climatic shifts, and global warming are all results of our over usage of these gases. An increasing number of people are turning to EV technology as a means of mitigating these consequences. Since electric vehicles are mostly made up of a battery system, powered electronic circuits, and an electric machine, they have a far lower fuel cost than their fossil fuel counterparts. When it comes to regulating how long a charge takes and how far it can take you, the battery pack in an electric vehicle is the single most important factor [1,2]. Because of the regenerative breaking function, electric machines in EVs may be run in generator mode as well as motor mode, a capability that is not achievable in traditional internal
combustion engine (ICE) cars. Therefore, during regenerative braking, the electric machine operates in generator mode, recharging its batteries [3,4]. All-electric cars (EVs) and hybrid electric vehicles (HEVs) are the two broad categories of EVs. Among the typical uses of electricity in households and businesses, recharging electric vehicles stands out. Due to the relatively high-power levels needed for such applications, DC-DC converter-based power conditioning solutions are a must. Dc / dc converter used during EV charging systems should fulfil the following criteria: high reliability, highly efficient, fault tolerance, and cheap cost. Vehicle-to-grid (V2G) services are predicted to become widespread in the near future, and the ability of EV chargers to offer bidirectional power is a crucial enabler of these services. Multiple DC-DC converter topologies used in Evs applications have been mentioned in the literature [6, 7]. Almost all of these DC-DC converters provide reactive power compensation, charging control, and/or galvanic isolation features as part of inter power conditioning systems, given the popularity of Central air energy distribution channels [8]. There are two main topologies that are favoured for use in non-isolated DC-DC converters. A number of studies [9–12] recommend using interleaved DC-DC converters for EV charging applications, whereas others [13–15] favour using multi-level DC-DC converters. When it comes to HEVs, you may choose between parallel and series models [5]. Parallel HEVs have an internal combustion engine (ICE) and an electric machine (EM) installed in the same chassis. During acceleration of an electric machine, while the cars are operating in electric mode, the motor is powered by a battery [6]. Alternatively, an all-electric vehicle has a battery, a power electronic
As may be observed in Fig. 1, a circuit and electric machine. When compared to HEVs and traditional ICE vehicle technology, the electric machine is the most environmentally friendly option since it eliminates gas emissions [3].In this investigation, we use MATLAB Simulink to model an EV system consisting of a battery, a bidirectional dc-dc converter, and a fuzzy logic controller (FLC). To further boost overall system efficiency, this converter design incorporates snubber capacitors in parallel

ISSN PRINT 2319 1775 Online 2320 7876

Research paper **Volume 10, Iss 3, 2021**

with the IGBTs. ANNs trained with supervised and unsupervised learning may recognise the converter's dataset and provide accurate results with little error. Based on the conversion efficiency maps generated by ANN algorithms as well as the resulting categorization of input voltages, the optimal voltage source may be selected in this manner

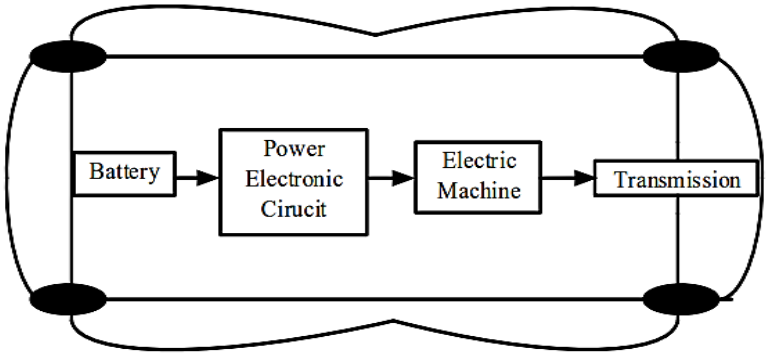

Fig.1.General Electric vehicle

To better forecast adaptive dc-link voltage, a novel control approach is presented in this study, which employs an ANN algorithm. This approach utilises the predictive & adaptive abilities of ANNs to quickly estimate the standard dc-link voltage. The suggested system also incorporates the other supervised or unsupervised control techniques. The suggested controller's performance is then compared to that of other ANN algorithm control strategies.

II SYSTEMDESCRIPTION

Battery, bidirectional dc-dc converter, floating-lead rectifier (FLC), and dc machine are the four components that make up the EV motor driver design. Figure 2 shows the Circuit diagram for EV machines.

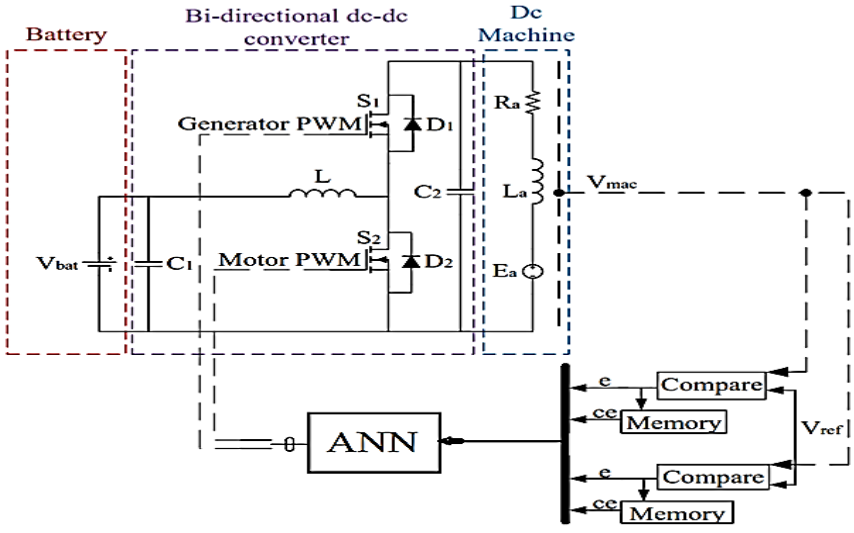

Fig.2.Circuit diagram for EV machines

The traction system in this research uses a dc machine with an operational voltage of 500 V dc, and the beginning voltage of the battery was set to 378 V. In generator mode, a bidirectional dc-dc converter may boost battery voltage to 500 V. When a dc supply is started at high speed, the acceleration drains the battery. The state of charge (SoC), flow, voltage, and dc machine voltage of a battery are monitored while simulating the motor mode with varying torque values. Duty cycles of S1 & S2 are set by the ANN to guarantee proper battery charging and discharging.

ISSN PRINT 2319 1775 Online 2320 7876
Research paper Volume 10, Iss 3, 2021

The components of a direct current (dc) machine are the brush, actuator core & copper coils, commutator, fields core and windings. The armature circuit consists of an inductor, a resistor, and a counter-electromotive source connected in series. In the generation mode simulation, battery metrics as SoC, current, voltage, and dc machine voltage are examined in relation to different dc machine torques. Table I details the technical aspects of the batteries.

TABLEI.BATTERYPARAMETERS

Parameter	Value
Battery Type	Lithium-ion
Nominal Voltage	350 V
Maximum Capacity	100 Ah
Exponential Voltage	378 V
Initial State of Charge	% 88
Cut off Voltage	262.5 V
Fully Charge Voltage	407.4 V
Nominal Discharge Current	44.5 A

III DESIGNOFEVMACHINEDRIVER

Dc Machine, A. A dc machine, working in accordance with the electromechanical energy conversion hypothesis, may change electrical energy into mechanical energy or vice versa [7]. The mode of operation of a generator is defined by the voltage induced on a conductor as it is moved inside a magnetic field. The motor mode works because a magnetic field is formed when an alternating current flows through a conductor. Torque is increased when a dc motor is started in an accelerating fashion. However, when used as a generator, the dc machine produces a negative torque [8, 9]. Four equations may be used to represent the mechanical equivalent of a dc machine. Dc machine voltage is given by (1)where KE is the voltage constant and is the dc machine speed, and KE is determined by (2)where Laf is the filament reciprocal field and If is the field current [12-13];

$$E = K_E.\omega \quad (1)$$

$$K_E = L_{af}.I_f \quad (2)$$

Where KT is the torque constant and Ia is the armature current, we get the formula for calculating an electromechanical torque (TE).

$$T_E = K_T.I_a \quad (3)$$

Constant dc machines generate both mechanical and electromagnetic torque. Torque applied to a DC machine is denoted by the symbol TL.

For the purpose of (4) [12-13], we define J to be the moment of inertia, Bm to be the friction coefficient, and Tf to be the coulomb friction torque.

$$J\frac{dw}{dt} = T_E - T_L - B_m.\omega - T_f \quad (4)$$

Using these equations, we may construct a dc machine using the parameters shown in Table II.

TABLEII.DCMACHINEPARAMETERS

Parameter	Value
Armature Voltage	500 V
Field Voltage	300 V
Machine Power	250 Hp

Bi-directionalDC-DCconverter

The voltage and current levels needed by the electric machine and the battery are converted via a bidirectional dc-dc converter. When switching between motor and generator modes, electric current flows in the opposite direction. A motor's acceleration is directly proportional to the amount of current it receives from its battery

ISSN PRINT 2319 1775 Online 2320 7876
Research paper Volume 10, Iss 3, 2021

pack during operation. On either hand, while operating in generator mode, the machine's output current must be transferred to the battery bank to replenish its power supply [9-12]. Accordingly, the device and controller architecture for the suggested bi-directional converter are developed in this study. Fig. 4 is a schematic representation of the core bidirectional converter. It consists of an inductor, two capacitors, two power diodes, and two switches (S1 and S2) (L).

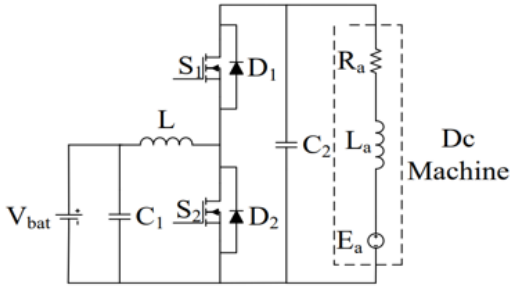

Fig.3.Fundamental circuit of bidirectional dc-dc converter

The bidirectional dc-dc converter is tested using the switching devices (S1, S2) and power diodes in both their on and off modes (D1, D2). The many ways of functioning are broken down as follows.

IVPROPOSEDANN-BASEDCONTROLSTRATEGY

To mimic the behaviour of a genuine neural network, ANNs mimic the structure of such networks by using one or even more hidden layers, each of which contains one or more neurons. For the purposes of this investigation, a kind of artificial neural network known as a feed-forward ANN (or FF-ANN) was utilised. In FF-ANN, information flows solely forward. Mathematical expression for such output of the a single neuron

$$y = \mathrm{Act}\left(b + \sum_{i=1}^{M} x_i w_i\right) \quad (5)$$

Where Act(.) is the activation function, wi are the weights of each input xi, b is the bias or correcting factor, and M is the number neural input units (or neurons) with characteristics x = x1, x2,..., xM. In Table I, we list the most prevalent forms of activation functions. An FF-ANN layer may be created by combining numerous neuronal networks into a single one. Multi-input, single-output FF-ANN may be described by the following generic equation:

$$y_1 = Act\left(\sum_{j=1}^{J} {}^{2}w_{j1} h_j + {}^{2}b_1\right) \quad (6)$$

$$h_j = Act\left(\sum_{m=1}^{M} {}^{1}w_{mj} x_m + {}^{1}b_j\right), \quad \forall j = \{1,\ldots,J\}, \quad (7)$$

wherein y1 is the outcome of the ANN, (1wmj, 2wj1) is the weight of the hidden layer, J is the amount of hidden units, Denotes the number million input nodes, and (1 bj, 2 b1) is the bias of the hidden layer and the output layer.

ISSN PRINT 2319 1775 Online 2320 7876
Research paper Volume 10, Iss 3, 2021

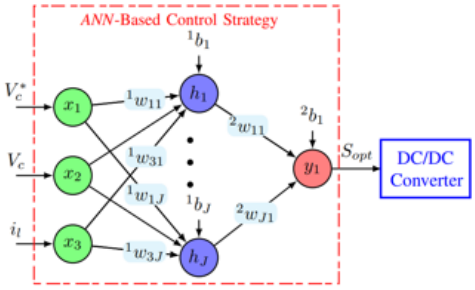

Fig.4.The ANN-based control approach

The ANN-based control approach presented in this work is shown in Figure 4. The precision of MPC is tied to how well the system is modelled mathematically. The suggested control technique, however, does not rely on the system model but rather on the training dataset. Input characteristics are transformed into the required outputs in a one-to-one correspondence. As a result, the ANN's effectiveness is independent of the details of the underlying system model. In this study, the optimum switching phase Sopt is assumed to be the aim or output of the trained Karen control scheme, while the references voltage V c, battery voltage Vc, and current il are selected as the input characteristics. First, input characteristics and their related outputs (input-output pairs) are extracted by a simulation of the MPC method. Once the information has been retrieved, it is utilised to teach the ANN. Three thousand and one are the total sampling rate used for training. At time instant k, the following is a summary of the control loop for the proposed Karen control strategy:
First, take a reading of il and Vc at time k.
The suggested controller uses the aforementioned variables and the set point V c to make an inference about the future switching state Sopt.
Thirdly, without utilising a modulator, the ideal switching state is applied to the converter. The optimal 15-neuron design is selected using a mesh refinement tuning strategy.
The ANN is trained and its biases and weights are fine-tuned using the bayesian regularised approach (BRT). With BRT, you may save time and effort on tedious cross-validation, which is a common practise in traditional propagation techniques [21-29]. Sixty percent of the randomized input data is utilised to training the ANN, while the remaining twenty percent is split between testing and validation. The entire confusion matrix for assessing the trained ANN's precision is shown in Figure 5. The diagonal elements of a matrix indicate the right categorization of the data class, while the other elements show the wrong classification. The trained ANN utilised in this research had a 97-percent accuracy rate. After the ANN model has been trained, it is brought into Simulink to see how well it does in the initial setting. In conclusion, the essential processes of the development and test phases of the having to learn control method are shown in Fig. 6.

V SIMULATIONRESULTS

The voltage of a dc machine is displayed in Fig.14, and the present, voltage, and SoC of the battery are given in Fig.5. Fig.6 displays the torque values of the motor and generator. The first 25 minutes of the dc machine's run time are spent in motor mode, while the latter 25 seconds are spent in generator mode. The switching pulse for the semiconductor switch is formed by comparing the duty ratio that was generated by the ANN with the switching frequency of a triangle waveform. The dc machine's voltage is lowered to the set point. Variable torque values lead to a rise in battery voltage and system on chip (SoC) performance. When the absolute value of torque is raised, the battery's state of charge (SoC), voltage, and current all rise accordingly. However, when the absolute magnitude of torque is dropped, the battery's state-of-charge (SoC), voltage, and current are all reduced.

Battery current, voltage & SoC are displayed in Fig.5 whereas motor and generating torque value are given in Fig. 5 and voltages of the dc machine is presented in Fig.6 The power generator is run during that first 25 seconds in engine mode and final 25 seconds in electrical form.

ISSN PRINT 2319 1775 Online 2320 7876
Research paper Volume 10, Iss 3, 2021

Fig. 5. a) Battery voltage b) battery current

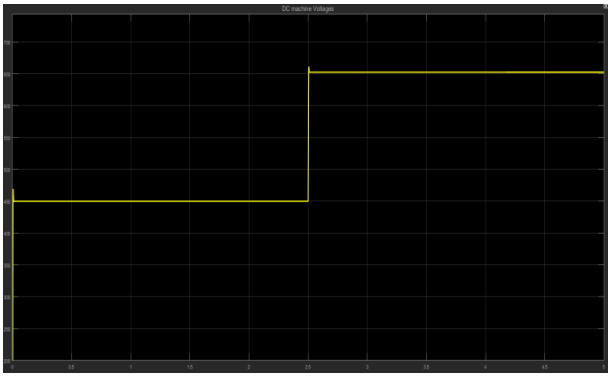

Fig. 6. Voltage of dc machine

VI CONCLUSION

The article describes the steps taken to develop and regulate a bidirectional dc-dc converter for use in an electric vehicle. Rules are implemented in FLC for controlling the bidirectional dc-dc converter. At low battery levels, the dc machine switches to motor mode, and the bidirectional dc-dc converter switches to boost mode. The dc motor's battery life is monitored while positive torque values of varying magnitudes are applied to the motor. It's great that the ANN were able to figure out how batteries work on its own. It may be used with many battery chemistries without the need for extensive engineering to develop new battery models. These precise outcomes were accomplished using a Neural Network design that was surprisingly simple. Following offline training, the network may be placed into a neural network chip, where the SOC can be approximated quickly using the four simple inputs. The simulation results show that the battery SoC drops from 88 percent to 87.88 percent while the dc machine voltage stays constant at 500 volts. At the time of battery charging, the dc machine is put into generator mode, and the bidirectional dc-dc converter is put into buck mode. The impact on the batter is

ISSN PRINT 2319 1775 Online 2320 7876
Research paper **Volume 10, Iss 3, 2021**

measured as low power values are given to the dc motor. Simulation results show that battery SoC improves from 87.337 to 97.345.

REFERENCES

[1] F. Zhang, X. Zhang, M. Zhang and A. S. E. Edmonds, "Literature review of electric vehicle technology and its applications," 2016 5th International Conference on Computer Science and Network Technology (ICCSNT), Changchun, 2016, pp. 832-837.

[2] Tiwari and O. P. Jaga, "Component selection for an electric vehicle: A review," International Conference on Computation of Power, Energy Information and Commuincation (ICCPEIC), Melmaruvathur, 2017, pp. 492-499.

[3] Jia Ying Yong, Vigna K. Ramachandaramurthy, Kang Miao Tan, N. Mithulananthan, "A review on the state-of-the-art technologies of electric vehicle, its impacts and prospects," Renewable and Sustainable Energy Reviews, vol: 49, 2015, pp: 365-385

[4] X. Nian, F. Peng and H. Zhang, "Regenerative Braking System of Electric Vehicle Driven by Brushless DC Motor," in IEEE Transactions on Industrial Electronics, vol. 61, no. 10, pp. 5798-5808, Oct. 2014.

[5] Yanzhi Wang, Xue Lin, M. Pedram and N. Chang, "Joint automatic control of the powertrain and auxiliary systems to enhance the electro mobility in hybrid electric vehicles," 2015 52nd ACM/EDAC/IEEE Design Automation Conference (DAC), San Francisco, CA, 2015, pp. 1-6.

[6] J. Zhang, T. Shen, Receding Horizon "Optimal Control of PHEV with Demanded Torque Estimation Model," IFAC-PapersOnLine, Volume 51, vol: 31, 2018, pp: 183-187 .

[7] Veeraiah N, Krishna BT. Intrusion detection based on piecewise fuzzy C-means clustering and fuzzy Naïve Bayes rule. Multimedia Research. 2018 Oct;1(1):27-32

[8] Z. Haishui, W. Dahu, Z. Tong and H. Keming, "Design on a DC Motor Speed Control," 2010 International Conference on Intelligent Computation Technology and Automation, Changsha, 2010, pp. 59- 63.

[9] S. J. Chapman, Electric Machine Fundamentals. New York: McGrawHill, 2005.

[10] J. Shen and A. Khaligh, "An energy management strategy for an EV with two propulsion machines and a hybrid energy storage system," IEEE Transportation Electrification Conference and Expo (ITEC), Dearborn, MI, 2015, pp. 1-5.

[11] M. S. Perdigão, J. P. F. Trovão, J. M. Alonso and E. S. Saraiva, "Large-Signal Characterization of Power Inductors in EV Bidirectional DC–DC Converters Focused on Core Size Optimization," IEEE Transactions on Industrial Electronics, vol. 62, no. 5, 2015, pp. 3042-3051.

[12] L. Albiol-Tendillo, E. Vidal-Idiarte, J. Maixé-Altés, J. M. BosqueMoncusí and H. Valderrama-Blaví, "Design and control of a bidirectional DC/DC converter for an Electric Vehicle," 15th International Power Electronics and Motion Control Conference (EPE/PEMC), Novi Sad, 2012, pp.2-5.

[13] I. Azizi and H. Radjeai, "A bidirectional DC-DC converter fed DC motor for electric vehicle application," 4th International Conference on Electrical Engineering (ICEE), Boumerdes, 2015, pp. 1-5.

[14] R. Cipin, M. Mach, M. Toman and J. Knobloch, "Measurement and evaluation of DC motor starting torque," 2017 IEEE International Conference on Environment and Electrical Engineering and 2017 IEEE Industrial and Commercial Power Systems Europe (EEEIC / I&CPS Europe), Milan, 2017, pp. 1-5.

[15] Premananda P., Singh R.K, Tripathi R.K. "Bidirectional DC-DC converter fed drive for electric vehicle system," International Journal of Engineering, Science and Technology vol. 3, no. 3, 2011, pp. 101- 110.

[16] R. H. G. Tan and L. Y. H. Hoo, "DC-DC converter modeling and simulation using state space approach," 2015 IEEE Conference on Energy Conversion (CENCON), Johor Bahru, 2015, pp. 42-47.

[17] Modabbernia, M. R., Sahab, A. R., Mirzaee, M. T., &Ghorbany, K. "The State Space Average Model of Boost Switching Regulator Including All of the System Uncertainties," Advanced Materials Research, vol: 403, 2012, pp: 3476–3483.

[18] M. S. Perdigão, J. P. F. Trovão, J. M. Alonso and E. S. Saraiva, "Large-Signal Characterization of Power Inductors in EV Bidirectional DC–DC Converters Focused on Core Size Optimization," in IEEE Transactions on Industrial Electronics, vol. 62, no. 5, 2015, pp. 3042-3051.

[19] Suresh, K., and R. Arulmozhiyal. "Design and Implementation of BiDirectional DC-DC Converter for Wind Energy System," Circuits and Systems, vol: l7 2016 pp: 3705-3722.

[20] R. Bayindir, I. Colak, E. Kabalci and E. Irmak, "The Fuzzy Logic Control of a Multilevel Converter in a Variable Speed Wind Turbine," 2009 International Conference on Machine Learning and Applications, Miami Beach, FL, 2009, pp. 787-790.

[21] Oscar Cordón, "A historical review of evolutionary learning methods for Mamdani-type fuzzy rule-based systems: Designing interpretable genetic fuzzy systems," International Journal of Approximate Reasoning, Volume 52, Issue 6,2011, pp 894-913.

[22] U. Srilakshmi, N. Veeraiah, Y. Alotaibi, S. A. Alghamdi, O. I. Khalaf and B. V. Subbayamma, "An Improved Hybrid Secure Multipath Routing Protocol for MANET," in IEEE Access, vol. 9, pp. 163043-163053, 2021, doi: 10.1109/ACCESS.2021.3133882.

[23] N. Veeraiah et al., "Trust Aware Secure Energy Efficient Hybrid Protocol for MANET," in IEEE Access, vol. 9, pp. 120996-121005, 2021, doi: 10.1109/ACCESS.2021.3108807.

[24] eeraiah, N., Krishna, B.T. Trust-aware FuzzyClus-Fuzzy NB: intrusion detection scheme based on fuzzy clustering and Bayesian rule. Wireless Netw 25, 4021–4035 (2019).

[25] Veeraiah, N., Krishna, B.T. An approach for optimal-secure multi-path routing and intrusion detection in MANET. Evol. Intel. 15, 1313–1327 (2022).

[26] N. Veeraiah and B. T. Krishna, "Selfish node detection IDSM based approach using individual master cluster node," 2018 2nd International Conference on Inventive Systems and Control (ICISC), 2018, pp. 427-431, doi: 10.1109/ICISC.2018.8399109.

[27] U. Srilakshmi, S. A. Alghamdi, V. A. Vuyyuru, N. Veeraiah and Y. Alotaibi, "A Secure Optimization Routing Algorithm for Mobile Ad Hoc Networks," in IEEE Access, vol. 10, pp. 14260-14269, 2022, doi: 10.1109/ACCESS.2022.3144679.

[28] K. Pradeep and N. Veeraiah, "VLSI Implemetation of Euler Number Computation and Stereo Vision Concept for CORDIC based Image Registration," 2021 10th IEEE International Conference on Communication Systems and Network Technologies (CSNT), 2021, pp. 269-272, doi: 10.1109/CSNT51715.2021.9509639.

P. Kollapudi, S. Alghamdi, N. Veeraiah, Y. Alotaibi, S. Thotakura et al., "A new method for scene classification from the remote sensing images," Computers, Materials & Continua, vol. 72, no. 1, pp. 1339– 1355, 2022.